

Available online at www.sciencedirect.com**ScienceDirect**

Energy Procedia 63 (2014) 5577 – 5585

Energy

Procedia

GHGT-12

Impact of reservoir conditions on CO₂-brine relative permeability in sandstones

Catriona Reynolds^{a*}, Martin Blunt^a, Sam Krevor^a^aDepartment of Earth Science and Engineering, Imperial College, South Kensington Campus, London, SW7 2AZ

Abstract

We demonstrate experimentally, that the spatial distribution of fluids in the pore space is the primary control on CO₂ relative permeability, and that the importance of spatial heterogeneity in rock properties such as capillarity, porosity and permeability on fluid distributions is controlled by viscous forces. The importance of viscous forces during drainage core floods is evaluated using fluid viscosity as the varying parameter in CO₂-brine core floods, and flow rate in N₂-water core floods. A transition from a heterogeneous to a homogeneous displacement is observed with increasing viscous force applied to the core. During capillary dominated core flooding the relative permeability is sensitive to flow rate and viscosity. Homogeneous displacements have an invariant relative permeability and as such are a measure of the true relative permeability of the rock.

© 2014 The Authors. Published by Elsevier Ltd. This is an open access article under the CC BY-NC-ND license (<http://creativecommons.org/licenses/by-nc-nd/3.0/>).

Peer-review under responsibility of the Organizing Committee of GHGT-12

Keywords: Relative permeability; CO₂ storage; steady-state; core flood; heterogeneity

1. Introduction

In geologic CO₂ storage, the flow of CO₂ once injected and how much of the CO₂ can be trapped relies on the relative permeability of each phase. The flow and distribution of CO₂ in the pore-space is controlled by CO₂-brine interfaces and fluid properties such as viscosity, density and interfacial tension (IFT). In oil-brine systems, the relative permeability is known to depend on the IFT only at values less than 1 mN m⁻¹ [1-3], and has been shown to

* Corresponding author. *E-mail address:* catriona.reynolds11@imperial.ac.uk

be independent of [4], or to increase with [5,6] viscosity ratio. The effect on CO₂-brine systems is unknown [7]. However, there is some evidence from modeling that the efficiency of CO₂ displacing brine is strongly dependent on flow rate, capillarity and gravity in the presence of heterogeneity [8,9]. Characteristic curves for relative permeability are a fundamental input to reservoir simulators that can be used both to history match and to design storage projects. Hence, accurate measurements of relative permeability at the conditions relevant to CO₂ storage are vital to be able to predict the migration of a plume of CO₂ once injected into the subsurface and the volumes of CO₂ that can be trapped by capillary snap-off. Despite increased interest in CO₂ storage, the response of the CO₂-water relative permeability to varying IFT has yet to be comprehensively evaluated.

We present the results of a programme of steady-state, horizontal core floods investigating the impact of fluid properties such as interfacial tension, viscosity ratio and density contrast on relative permeability. Drainage relative permeability curves for CO₂-brine and N₂-water were measured at conditions applicable to storage of supercritical CO₂ (8-25 MPa, 35-120°C and 0-5 mol kg⁻¹). The pressure, temperature and brine salinity conditions were selected to provide a wide range of fluid properties, which may impact relative permeability. Of particular concern were interfacial tension (29-49 mN m⁻¹), viscosity ratio μ_{CO_2}/μ_{brine} (0.03-0.12) and density contrast ρ_{brine}/ρ_{CO_2} (1.2-7.1). The work was performed in a high pressure, high temperature core flooding and x-ray imaging facility purpose built for the investigation of multiphase flow and CO₂ storage. Experiments were performed on a single Bentheimer sandstone core, using a comprehensive suite of core flood techniques, combining traditional steady state and novel techniques to obtain permeabilities at high CO₂ saturations. In situ fluid saturations were measured using an X-ray CT scanner.

Nomenclature

μ	viscosity (Pa s)
ρ	density (kg m ⁻³)
M	viscosity ratio (μ_{CO_2}/μ_{brine})
D	density contrast (ρ_{brine}/ρ_{CO_2})
Ca_{max}	maximum capillary number
ϕ	porosity
k	absolute permeability (D)
L	length of core (m)
A	cross-sectional area (m ²)
V_p	pore volume (ml)
q_T	total flow rate (ml/min)
q_w	flow rate of water/ wetting phase (ml/min)
$q_{N_2,co_2,nw}$	flow rate of non-wetting phase (ml/min)
f_{N_2,co_2}	Fractional flow of non-wetting phase (q_{nw}/q_T)

2. Experimental method

2.1. Pressure, temperature, salinity and flow rates for CO₂-brine and N₂-water core floods

The experimental conditions were chosen so as to represent the range of interfacial tensions that may be encountered for geological storage for supercritical CO₂ in a typical saline aquifer ($T_{crit} = 31^\circ\text{C}$, $P_{crit} = 7.4$ MPa), while being able to isolate any change due to varying an individual fluid parameter. Temperature and pressure conditions for the storage of supercritical CO₂ at depths of ~0.8 to 3 km range from 32 to 120°C and 7.5 to 30 MPa [10]. The change in fluid properties such as viscosity and IFT with pressure, temperature and salinity in the CO₂-brine system are well known [11-13]. Interfacial tension varies from 25 to 55 mN m⁻¹, while viscosity ratio, $M = \mu_{CO_2}/\mu_{brine}$, ranges from 0.02 to 0.2, with most of the change coming from μ_{CO_2} [10, 14]. Conditions may be easily selected to obtain a range of interfacial tensions.

To isolate the independent impact of IFT and viscosity on relative permeability, conditions for CO₂-brine core floods were selected along lines of constant viscosity ratio, varying density ratio and/ or IFT (Figure 1, Table 1 and Table 2). All N₂-water core floods were performed at the same pressure and temperature, while varying total flow rate, and the fractional flow of N₂ (Table 3).

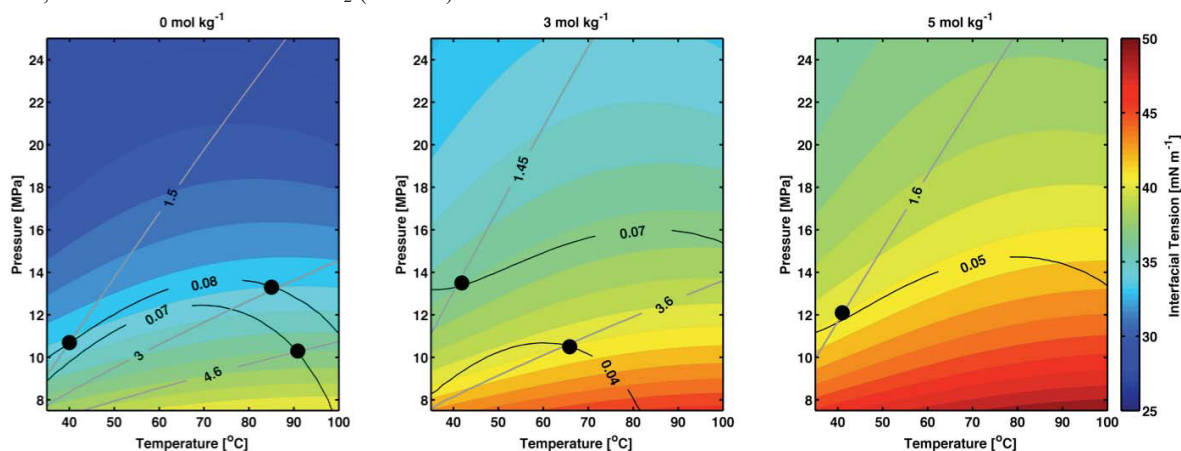


Figure 1. Pressure-temperature-IFT graphs for CO₂-brine core floods. IFT values calculated for 0, 3 and 5 mol kg⁻¹ NaCl brine molality [11]. Grey lines of constant density ratio, black lines of constant viscosity ratio and black circles denote core flood conditions.

Table 1. Experimental conditions of Bentheimer core floods.

Experiment	Fluids	P (MPa)	T (°C)	S (mol kg ⁻¹)	IFT ^a (mN m ⁻¹)	q _T (ml/min)
1	N ₂ -DI	15.5	50	0	62	5 - 75
2	CO ₂ -DI water	10.3	91	0	36.9737	20
3	CO ₂ -brine	13.5	42	3	36.9205	20
4	CO ₂ -brine	10.5	65	3	41.0009	20
5	CO ₂ -DI water	10.7	40	0	34.2359	20
6	CO ₂ -DI water	13.3	85	0	34.00073	20
7	CO ₂ -brine	12.1	41	5	40.9694	20









^aCO₂-DI water and CO₂-brine IFT calculated from [11].

Table 2. Fluid properties of core floods.

Experiment	Fluids	Viscosity (Pa s)		Density (kg m ⁻³)		M	D	Ca _{max} ^b	
		CO ₂	brine	CO ₂	brine			CO ₂	brine
1	N ₂ -DI	0.0000221	0.0005498	155.0	996.5	0.04	6.43	4.7 x 10 ⁻⁷	1.2 x 10 ⁻⁵
2	CO ₂ -DI water	0.0000221	0.0003140	209.9	963.4	0.07	4.59	7.9 x 10 ⁻⁷	1.1 x 10 ⁻⁵
3	CO ₂ -brine	0.0000613	0.0008682	736.1	1078.7	0.07	1.47	2.3 x 10 ⁻⁶	3.1 x 10 ⁻⁵
4	CO ₂ -brine	0.0000243	0.0006088	292.0	1064.0	0.04	3.64	7.8 x 10 ⁻⁷	2.0 x 10 ⁻⁵
5	CO ₂ -DI water	0.0000527	0.0006539	671.7	1003.5	0.08	1.49	2.0 x 10 ⁻⁶	2.5 x 10 ⁻⁵
6	CO ₂ -DI water	0.0000270	0.0003374	329.7	968.7	0.08	2.94	1.0 x 10 ⁻⁶	1.3 x 10 ⁻⁵
7	CO ₂ -brine	0.0000577	0.0011206	711.2	1132.1	0.05	1.59	1.9 x 10 ⁻⁶	3.6 x 10 ⁻⁵

^bCa_{max} calculated at q_T = 20 ml/min using $v\mu_i/\phi\sigma$ where v is the total Darcy fluid velocity in m s⁻¹, μ_i is the fluid viscosity in Pa s, ϕ the porosity and σ the interfacial tension.

Table 3. Flow parameters for CO₂-brine and N₂-water core floods. Bold indicates parameter held constant throughout experiment.

Symbol	  					
f_{nw}	0.0013 – 0.9999	0.0155 – 0.99994	0.1426 – 0.99286	0.025 – 0.995	0.83342 – 0.991	0.54762 – 0.81
q_{nw}	0.026 – 19.998	0.099 – 19.989	1.00 – 6.95	1.0 – 39.8	3.377 – 74.301	11.5 – 40.5
q_w	19.974 – 0.002	19.901 – 0.011	6.00 – 0.05	39.0 – 0.2	0.675	9.5
q_T	20	20	7	40	4.052 – 74.976	21 – 50

2.2. Rock core

Experiments are performed on a Bentheimer sandstone core (Table 4), composed of >95% quartz with minor feldspars and clays. The core was selected for its simple heterogeneity (Figure 2) in pore structure and unreactive mineralogy and is expected to be strongly water-wet. All experiments are carried out on the same core.

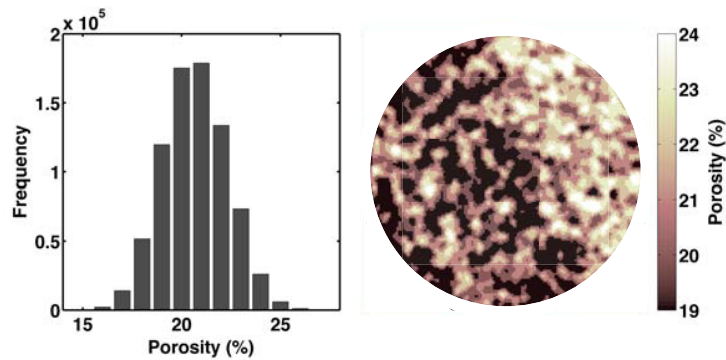


Figure 2. (L) CT-measured porosity of Bentheimer core. (R) Representative slice through rock core showing porosity heterogeneity.

Table 4. Properties of Bentheimer rock core.

$\phi^{c,d}$	k^d (D)	L (m)	A (m ²)	V_P^c (ml)
0.222 ± 0.019	1.81 ± 0.12	0.239	0.00112	59.4

^c X-ray CT measured porosity. ^d Averaged over 7 core floods.

2.3. Flow loop

Core flood are conducted in a high pressure, high temperature, corrosion-resistant flow loop (Figure 3). Dual CO₂/ N₂ and brine pumps are used to co-circulate fluids. Automatic valve packages control the flow and refill of the pumps. Fluids are circulated through a horizontal core holder, to a custom-built two-phase separator from which they are returned to the pumps. A back pressure pump on the outlet side of the core is used to maintain the system pressure and a confining pump applies an overburden of 5 MPa over the experimental pressure to the core. All flow lines and pumps are constructed from a corrosion resistant alloy (Hastelloy). All flow lines, pumps, the separator and core holder are heated using a heating lines, ovens or heating baths where appropriate. The core holder is constructed from aluminium, which is transparent to x-rays, and placed inside a medical X-ray CT scanner.

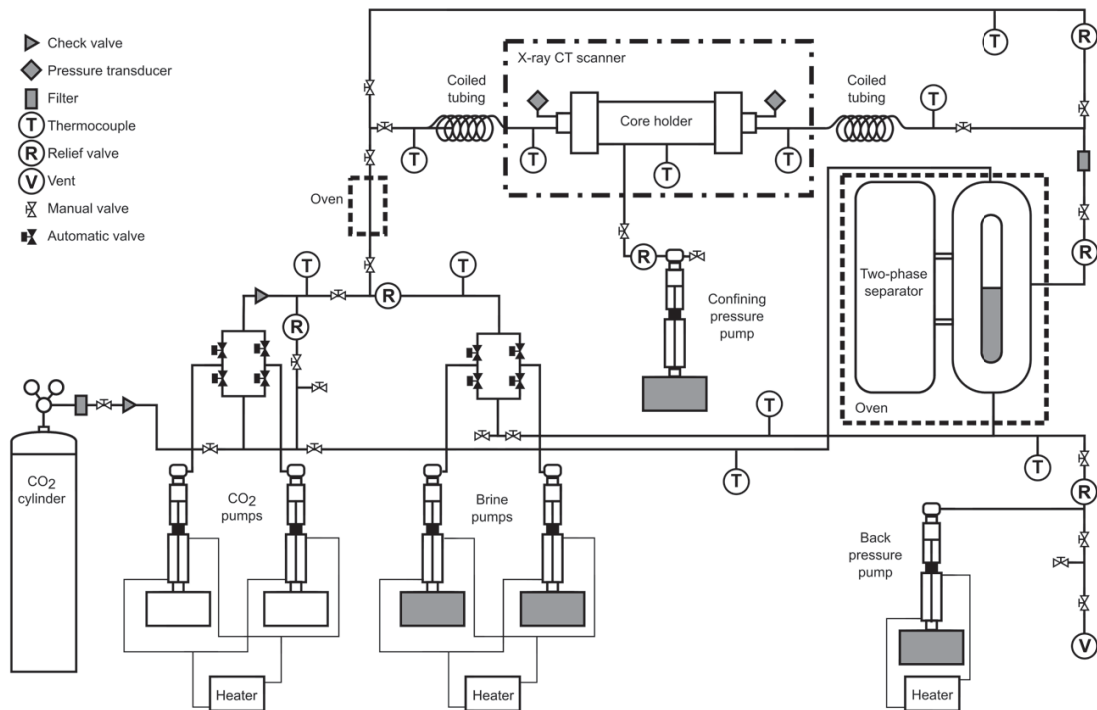


Figure 3. Schematic of flow loop for CO₂-brine horizontal core floods

2.4. Measuring Drainage Relative Permeability

Relative permeability is measured using the steady-state method [15-18]. Supercritical CO₂ and brine are co-circulated overnight, outside the core, so that both fluids are fully saturated with respect to one another, thus ensuring displacement during core-flooding is immiscible. This step is not necessary in N₂-water core floods. Pressure is measured at the inlet and outlet faces of the core. Fluids are circulated through the core until the fluid saturations reach steady state, i.e. there is a constant saturation profile along the length of the core, and the pressure drop across the core is stable. Saturation is measured using an X-ray CT scanner. Background scans of the core 100% saturated with CO₂/ N₂ and 100% saturated with brine are taken at experimental conditions prior to beginning a drainage experiment. These scans are used to calculate saturation during flow. To measure the primary drainage relative permeability, the fractional flow of CO₂ is increased stepwise from zero to 100%, until the maximum CO₂ saturation is achieved. The absolute permeability to brine is measured prior to the beginning of the drainage experiment by measuring the pressure drop across the brine-saturated core at a range of flow rates. Absolute permeability (*k*) is calculated using Darcy's equation for single-phase flow.

Under the conditions of a horizontal, steady state core flood, the relative permeability of each phase may be calculated using the multiphase extension to Darcy's Law [19],

$$q_i = - \frac{A k k_{r,i} S_i \Delta P}{\mu_i L},$$

where the cross-sectional area, *A*, and length, *L*, of the core, and absolute permeability *k* are measured prior to beginning the experiment. For each fluid phase (subscript *i*) the flow rate *q_i* is specified and viscosity *μ_i* is calculated for the experimental conditions. For each change in flow rate, the relative permeability *k_{r,i}* can be obtained from the measured pressure drop ($\Delta P = P_{inlet} - P_{outlet}$) across the core and in situ fluid saturation *S_i* is observed using the X-ray CT scanner.

3. Results and Discussion

3.1. CO₂-brine core floods

Drainage relative permeability curves were measured at a $q_T = 20$ ml/min for six CO₂-brine conditions and one N₂-water (Figure 4). Pairs of CO₂-brine experiments were performed at the same interfacial tension, but different fluid viscosities and densities (Figure 5). Heterogeneous displacements were produced at conditions of low CO₂ or N₂ viscosity and density, where the spatial distribution of the non-wetting phase is controlled strongly by the pore space heterogeneity (Figure 6). At high non-wetting phase viscosities a homogeneous displacement was produced, where the flow paths of the non-wetting phase are not controlled by the heterogeneity of the pore space, instead the non-wetting phase can access the whole rock core. Relative permeability to brine was found to be insensitive to changes in non-wetting phase viscosity. In contrast, relative permeability to CO₂ or N₂ was found to be constant during homogeneous displacements, but varied during heterogeneous displacements. Displacements with a homogeneous spatial distribution of CO₂ produced the highest CO₂ relative permeability and concurrently, the lowest irreducible water saturation.

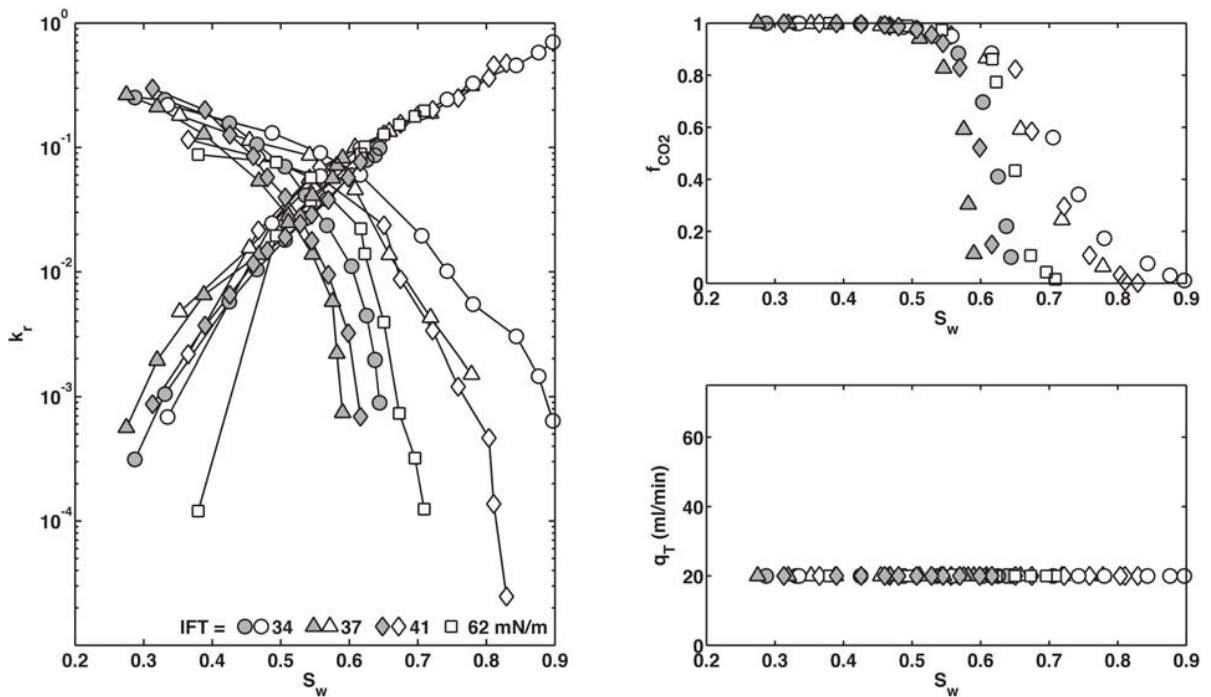


Figure 4. Steady state relative permeability (k_r), fractional flow of CO₂/N₂ (f_{CO_2}) and total flow rate (q_T) plotted against water saturation (S_w) for six CO₂-brine and one N₂-brine drainage core floods. Symbol types denote IFT (CO₂ = 34-41 mN/m and N₂ = 62 mN/m), grey symbols are homogeneous displacements, white symbols are heterogeneous displacements.

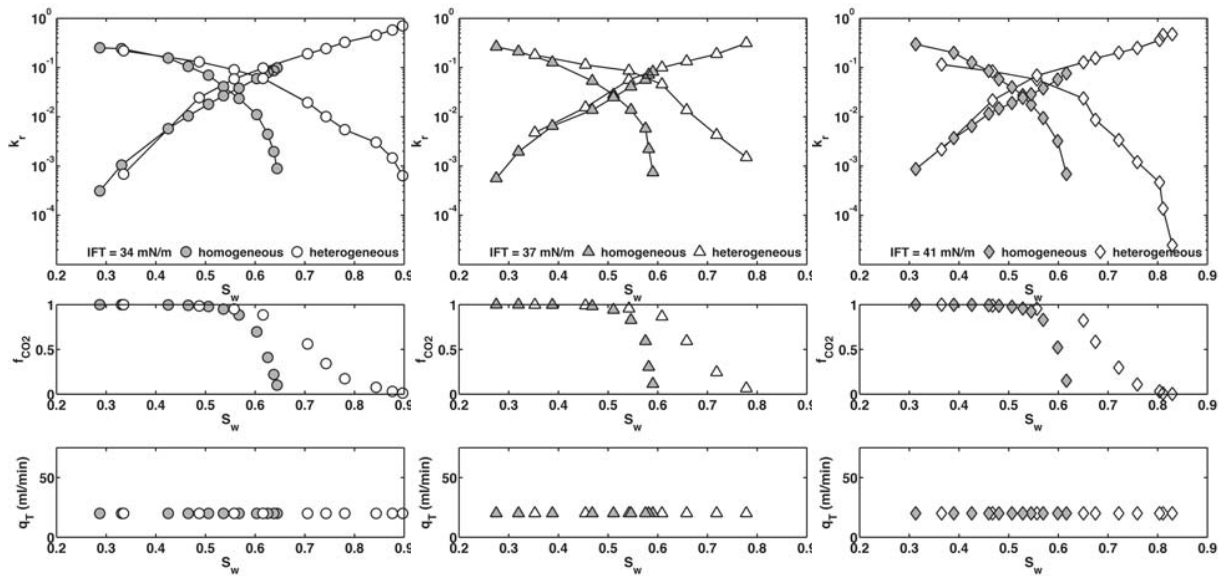


Figure 5. CO₂-brine core floods of the same interfacial tension are compared. Homogeneous displacements correspond to Experiments 3, 5 and 7 and heterogeneous to Experiments 2, 4 and 6 in Table 1.

f_{CO_2}	0.9501	0.9504	0.82705	0.95616	0.92285	0.9543	0.97445
q_{CO_2} (ml/min)	19.002	19.008	16.541	19.123	18.457	19.086	19.489
q_T (ml/min)	● 20	○ 20	▲ 20	△ 20	◆ 20	◇ 20	□ 20
S_w (%)	53.6	55.8	54.5	55.7	54.5	55.7	54.4

Figure 6. Comparison of CO₂-brine fluid distribution during steady state core floods. Slices shown at ~12.5 cm from inlet of core. Fluid saturation is measured by an X-ray CT scanner. Each slice has a diameter of 148 pixels, and a voxel resolution of .25 x .25 x 1 mm. Dark red indicates the pore space is completely filled by CO₂ ($S_w = 0$), dark blue indicates pore space is completely filled by brine ($S_w = 1$). Colours in between indicate pores within an individual voxel contain both CO₂ and brine.

3.2. N₂-water core floods

Homogeneous or heterogeneous displacements can be produced at constant fluid viscosity by varying q_T . The transition from heterogeneous to homogeneous displacements during N₂-water core floods occurs at $q_T > 20$ ml/min. At low q_T both relative permeability to N₂ and water vary with flow rate. At high q_T relative permeability is constant (Figure 7 and Figure 8). If q_T is increased but q_w is held constant, there is no transition to the homogeneous displacement if q_w is low (Figure 9, $q_w = 0.675$ ml/min). As the displacement stays heterogeneous, each point on the relative permeability curve can be thought of as belonging to a different relative permeability curve, defined by the q_T (Figure 7, blue squares). However, if q_w is high (Figure 8, $q_w = 9.5$ ml/min), the displacement is homogeneous, and the same invariant relative permeability as for other homogeneous displacements is measured (Figure 7, black squares). Both q_T and q_w must exceed a critical value to achieve a homogeneous displacement and invariant relative permeability.

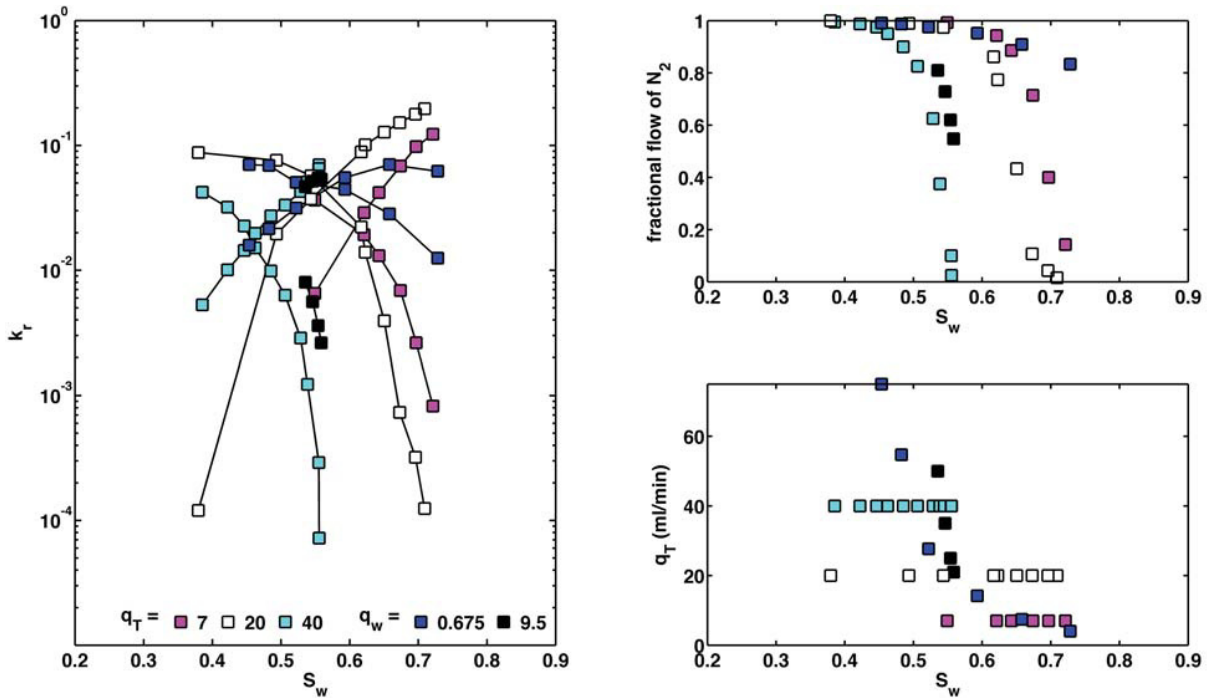


Figure 7. Drainage relative permeability (k_r), fractional flow of N_2 and total flow rate (q_T) plotted against water saturation (S_w) for N_2 -brine drainage core floods at a constant total flow rate or constant water flow rate (q_w).

f_{N_2}	0.943	0.511	0.54762	0.62	0.72857	0.1	0.81
q_{N_2} (ml/min)	6.6	19.489	11.5	15.5	25.5	4.0	40.5
q_T (ml/min)	7	20	21	25	35	40	50
S_w (%)	54.7	54.3	55.8	55.6	53.3	55.1	52.5

Figure 8. Comparison of N_2 -water fluid distribution at constant $q_T = 7, 20$ or 40 ml/min or constant $q_w = 9.5$ ml/min.

f_{N_2}	0.83342	0.90915	0.95241	0.97563	0.98766	0.991000
q_{N_2} (ml/min)	3.38	6.76	13.5	27.0	54.0	74.3
q_T (ml/min)	4.052	7.43	14.184	27.693	54.712	74.976
S_w (%)	73.8	66.1	59.0	52.0	49.4	45.3

Figure 9. Comparison of N_2 -water fluid distribution at constant $q_w = 0.675$ ml/min.

4. Conclusions

We have performed drainage core floods using CO₂-brine (varying viscosity) and N₂-water (varying total flow rate) on a single heterogeneous sandstone rock core. We find two types of displacement: a heterogeneous displacement, where flow of the non-wetting phase is dominated by the capillary heterogeneity in the core and relative permeability is controlled by total flow rate; and homogeneous displacements, where a high viscous pressure allows the non-wetting phase to invade the whole pore space and relative permeability is invariant.

Acknowledgements

The authors gratefully acknowledge funding from the Qatar Carbonates and Carbon Storage Research Centre (QCCSRC), provided jointly by Qatar Petroleum, Shell, and Qatar Science & Technology Park.

References

- [1] Amaefule JO, Handy LL. The Effect of Interfacial Tensions on Relative Oil/Water Permeabilities of Consolidated Porous Media. *Old SPE Journal* 1982; 22(3): 371-381.
- [2] Fulcher Jr RA, Ertekin T, Stahl CD. Effect of Capillary Number and Its Constituents on Two-Phase Relative Permeability Curves. *J Petrol Technol* 1985; 37(2): 249-260.
- [3] Bardon C, Longeron DG. Influence of Very Low Interfacial Tensions on Relative Permeability. *Old SPE Journal* 1980; 2: 391-401.
- [4] Leverett MC. Flow of oil-water mixtures through unconsolidated sands. *Trans AIME* 1939; 132(1): 149-171.
- [5] Yuster ST. Theoretical considerations of multiphase flow in idealized capillary systems. *Proceedings of the 3rd World Petroleum Congress, Section II, The Hague* 1951; 2: 437-445.
- [6] Odeh AS. The Effect of Viscosity Ratio on Relative Permeability. *Trans AIME* 1959; 216: 346-353.
- [7] Bachu S, Bennion B. Effects of in-situ conditions on relative permeability characteristics of CO₂-brine systems. *Environ Geol* 2008; 54(8): 1707-1722.
- [8] Kuo C-W, Perrin J-C, Benson SM. Effect of Gravity Flow Rate and Small Scale Heterogeneity on Multiphase Flow of CO₂ and Brine. *SPE Western Regional Meeting. Society of Petroleum Engineers*, 2010.
- [9] Kuo C-W, Benson SM. Analytical Study of Effects of Flow Rate Capillarity and Gravity on CO₂/Brine Multiphase-Flow System in Horizontal Corefloods. *SPE Journal* 2013; 18(4): 708-720.
- [10] Nordbotten JM, Celia MA, Bachu S. Injection and Storage of CO₂ in Deep Saline Aquifers: Analytical Solution for CO₂ Plume Evolution During Injection. *Transport in Porous Media* 2005; 58: 339-360.
- [11] Li X, Boek E, Maitland GC, Trusler JPM. Interfacial Tension of (Brines + CO₂): (0.864 NaCl + 0.136 KCl) at Temperatures between (298 and 448) K, Pressures between (2 and 50) MPa, and Total Molalities of (1 to 5) mol kg⁻¹. *Journal of Chemical & Engineering Data* 2012; 57: 1078-1088.
- [12] Fenghour A, Wakeham WA, Vesovic V. The Viscosity of Carbon Dioxide. *Journal of Physical and Chemical Reference Data* 1998; 27: 31-44.
- [13] Kestin J, Khalifa HE, Correia RJ. Tables of the Dynamic and Kinematic Viscosity of Aqueous NaCl Solutions in the Temperature Range 20-150°C and the Pressure Range 0.1-35 MPa. *American Chemical Society and the American Institute of Physics for the National Bureau of Standards* 1981; 1-17.
- [14] Adams JJ, Bachu S. Equations of state for basin geofluids: algorithm review and intercomparison for brines. *Geofluids* 2002; 2: 257-271.
- [15] Krevor S, Pini R, Zuo L, Benson SM. Relative permeability and trapping of CO₂ and water in sandstone rocks at reservoir conditions. *Water Resources Research* 2012; 48(2).
- [16] Perrin JC, Benson S. An experimental study on the influence of sub-core scale heterogeneities on CO₂ distribution in reservoir rocks. *Transport in porous media* 2010; 82(1): 93-109.
- [17] Honarpour MM, Koederitz F, Herbert A. *Relative permeability of petroleum reservoirs*. 1986.
- [18] Müller N. Supercritical CO₂-brine relative permeability experiments in reservoir rocks—Literature review and recommendations. *Transport in porous media* 2011; 87(2): 367-383.
- [19] Muskat M, Meres MW. *The Flow of Heterogeneous Fluids Through Porous Media*. *Physics* 1936; 7: 346-363.